Dalton Transactions

Diferrocenylmercury Diphosphine Diastereomers with Unique Geometries: trans-Chelation at Pd(II) with Short Hg(II)...Pd(II) Contacts

Journal:	*Dalton Transactions*
Manuscript ID	DT-ART-06-2019-002728.R1
Article Type:	Paper
Date Submitted by the Author:	13-Aug-2019
Complete List of Authors:	Tagne Kuate, Alain; Rutgers University Newark, Department of Chemistry Lalancette, Roger; Rutgers University Newark, Department of Chemistry Bannenberg, Thomas; Technische Universität Braunschweig, Institut für Anorganische und Analytische Chemie Tamm, Matthias; Technische Universität Braunschweig, Institut für Anorganische und Analytische Chemie Jaekle, Frieder; Rutgers University Newark, Department of Chemistry

Diferrocenylmercury Diphosphine Diastereomers with Unique Geometries: *trans*-Chelation at Pd(II) with Short Hg(II)···Pd(II) Contacts

Alain C. Tagne Kuate,[a,b] *Roger. A. Lalancette,*[a] *Thomas Bannenberg,*[c]

Matthias Tamm,[c] *and Frieder Jäkle*[a]*

[a] Department of Chemistry, Rutgers University-Newark,

73 Warren Street, Newark, NJ 07102, USA

[b] Department of Chemistry, Faculty of Sciences, University of Dschang,

P.O. Box 67, Dschang, Cameroon

[c] Institut für Anorganische und Analytische Chemie, Technische Universität Braunschweig,

Hagenring 30, 38106 Braunschweig, Germany

*To whom correspondence should be addressed. Email: fjaekle@rutgers.edu

Abstract. Diphosphine chelate ligands are essential in many catalytic processes with both the electronic structure and bite angle having a dramatic influence on the coordination behavior and catalytic performance. The synthesis of a new class of diferrocenylmercury-supported diphosphine chelate ligands was accomplished by the reaction of (*ortho*-diphenylphosphino)ferrocenyl sulfinate (**2**) with *t*-BuLi, followed by treatment with mercury(II) chloride. Two diastereomers, **4a** (p*S*p*R*-, *meso*-isomer) and **4b** (p*S*p*S*-isomer), differ in the orientation of the ferrocene moiety relative to the central $Ph_2PC_5H_3$-Hg-$C_5H_3PPh_2$ bridging entity. They were isolated independently and fully characterized in solution and in the solid state by single crystal X-ray diffraction analysis. Key characteristics of these ligands are their exceptionally wide and flexible bite angles and the unique stereochemical environment that is achieved upon coordination to transition metals. Complexation to Pd(II)Cl_2 gives rise to unusual square-planar *trans*-chelate complexes **5a** (*meso*) and **5b** (p*S*p*S*). In competition reactions, **4a** and **4b** show similar reactivity toward Pd(II)Cl_2. The molecular structures of **5a** and **5b** exhibit short Pd···Hg contacts, possibly indicating secondary metallophilic interactions as further evidenced by bond-critical points between Pd and Hg that were identified by AIM analyses.

Introduction

Bidentate diphosphine ligands play important roles in catalysis owing to the chelate effect that enhances the stability of metal complexes, as well as the tunability of electronic and steric effects.[1] The "bite angle" (β) is a characteristic geometric parameter that describes steric effects and can have a pronounced influence on the catalytic process.[2] Among the most commonly used ligands is DPEphos with a calculated natural β = 102.2° (Chart 1). In another example, the Xantphos ligand and related diphosphines favor *cis*-coordination to transition metals as they display limited flexibility due to the rigid heterocyclic backbone with bite angles in the range of ~100−134°.[2c, 3] At the other extreme, SPANphos (β ~ 172°) preferentially adopts a *trans*-configuration, and its rigid structure makes *cis*-complexation unfavorable.[4,5] *trans*-Coordination is also observed with recently introduced diphosphines based on a rigid *para*-terphenyl framework (TpPhos). In this case, the central Ph ring can undergo π-interactions with the metal center,[6] similar to the electron-donating effect of the oxygen atom in DPEphos.

Replacement of the σ-donating oxygen atom in DPEphos by σ-acceptor atoms such as boron, antimony or mercury results in Z-type diphosphine ligands (also referred to as ambiphilic ligands[7]). Depending on the Z-bridging atom, they behave either as *cis*- or *trans*-chelating ligands with natural bite angles between ~94−100° for the diphosphine-borane (DPB), ~166−170 for the diphosphine-stibine (DPSb), and ~172−176° for the diphosphine-mercury (DPHg).[8] In an interesting recent development, the trans-chelating diphosphine ligand (DBAphos) based on a diboraanthracene framework was applied in the synthesis of an anionic auride species, which is stabilized by donor-acceptor interactions with the boron centers.[9]

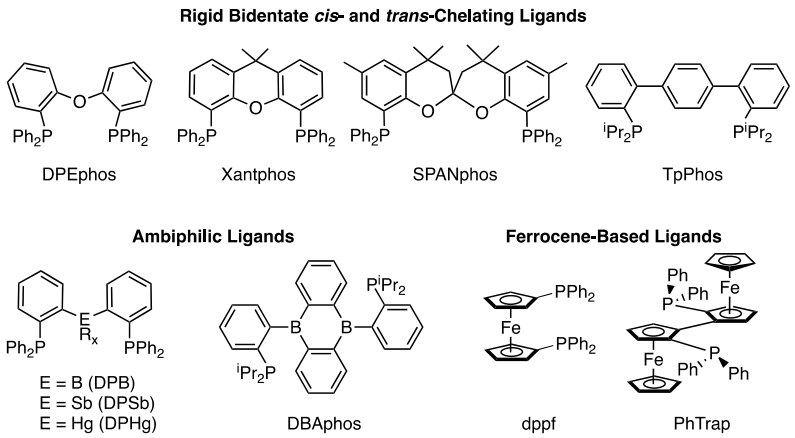

Chart 1. Examples of diphosphine chelate ligands.

Only very few diphosphine ligands are known that are truly flexible in that they accommodate both a *trans*- and *cis*-chelation mode. Among them is the chiral diphosphine PhTrap (β ~ 162°), which nicely illustrates the potential of ferrocene fragments[10] as building blocks for flexible diphosphine ligands.[11] Intriguingly, the insertion of a bridging σ-acceptor atom between the two ferrocenylphosphine moieties may turn PhTrap into a flexible Z-type ambiphilic diphosphine ligand with a highly variable bite angle that adopts to the specific geometric requirements during coordination to transition metals.

As part of our efforts to develop new ferrocene-based Lewis acids and Lewis pairs[12] we have recently introduced a first example of such a diphosphine ligand, (p*S*p*S*)-Hg(*ortho*-$FcPPh_2)_2$, with mercury acting as the bridging σ-acceptor atom.[13] A complex with $HgCl_2$ bound to the phosphines unexpectedly formed by successive Sn/Hg exchange reactions (β = 138.36(5)°),[14] and the corresponding free ligand ((p*S*p*S*)-**4b**; see Scheme 1) was isolated by $HgCl_2$ abstraction using cyanide. We anticipated that this new redox active and planar chiral diphosphine should exhibit a wide and flexible bite angle with unique stereochemical configuration, potentially resulting in broad adoption in transition metal coordination chemistries. In this work, we present a new

synthetic route that allows for facile isolation and structural characterization of both the *rac*- and *meso*-isomers of the ambiphilic diphosphine ligand Hg(*ortho*-$FcPPh_2)_2$. We compare the reactivity and coordination behavior of the individual isomeric ligands as exemplified in the formation of *trans*-chelated Pd(II) metal complexes and evaluate the presence of metallophilic interactions in the resulting mixed-metal complexes using computational methods.

Experimental Section

Materials. $HgCl_2$, *t*-butyllithium (1.7 M in pentane), and $PdCl_2$(COD) were purchased from commercial sources and used without further purification. The synthesis of (p*S*,S_s)-diphenylphosphinoferrocenyl sulfinate (**2**)[13, 15] has been previously reported.

Caution: Mercury compounds are highly toxic! Reactions involving mercury species have to be handled with extreme caution and the use of engineering barriers including non-permeable and resistant gloves is essential. Organolithium reagents and *t*-butyllithium in particular are highly reactive and need to be handled accordingly.

General Methods. All reactions were carried out under an atmosphere of dry nitrogen using high vacuum Schlenk-line techniques or an inert-atmosphere glove box (MBraun). Commercial-grade solvents (toluene, hexanes) were purified by a solvent purification system from Innovative Technologies, degassed and stored over sodium-potassium (NaK) alloy prior to use. Tetrahydrofuran was distilled from sodium/benzophenone and dichloromethane from CaH_2, degassed and stored under nitrogen atmosphere. 500.2/599.7 MHz ^{1}H NMR, 125.7/150.8 MHz ^{13}C NMR and 202.5 MHz ^{31}P NMR spectra were recorded on a Bruker Avance III HD NMR spectrometer (Bruker BioSpin, Billerica, MA) equipped with a 5 mm broadband gradient SmartProbe (Bruker, Billerica, MA) or a 600 INOVA NMR spectrometer (Varian Inc., Palo Alto,

CA) equipped with a 5 mm dual broadband gradient probe (Nalorac, Varian Inc., Martinez, CA). Chemicals shifts (δ) are given in ppm and were referenced internally to deuterated solvent signals ($CDCl_3$ 7.26 (^1H), 77.36 (^{13}C); C_6D_6 7.15 (^1H), 128.62 (^{13}C)). Coupling constants (J) are reported in Hertz (Hz) and splitting patterns are indicated as s (singlet), d (doublet), dd (doublet of doublets), pt (pseudo triplet), t (triplet), br (broad), nr (non-resolved) and m (multiplet), and the following abbreviations are used for signal assignments: Ph = phenyl, Fc = ferrocenyl, Cp = cyclopentadienyl, Me = methyl. High-resolution electrospray ionization-mass spectrometry (ESI-MS) and matrix-assisted laser desorption ionization-mass spectrometry (MALDI-MS) data were obtained on an Apex Ultra 7.0 Hybrid FTMS and MALDI-TOF (time-of-flight) MS data on a Bruker Ultraflextreme. Elemental analyses were performed by Quantitative Technologies Inc., Whitehouse, NJ.

Single crystal X-ray diffraction analysis. Reflections for *meso*-**4a**, *rac*-**4b**, *meso*-**5a**, and (p*S*p*S*)-**5b** were collected on a Bruker SMART APEX II CCD Diffractometer using CuKα (1.54178 Å) radiation at 100 K. Data processing, Lorentz-polarization, and face-indexed numerical absorption corrections were performed using SAINT, APEX, and SADABS computer programs.[16] The structures were solved by direct methods and refined by full-matrix least squares based on F^2 with all reflections using the SHELXTL V6.14 program package.[17] Non-hydrogen atoms were refined with anisotropic displacement coefficients. All H atoms were found in electron-density difference maps and treated as idealized contribution. Structural data have been deposited with the Cambridge Structure Database as supplementary publications CCDC 1935847-1935850.

Computational Studies: All computations were performed using the hybrid density functional method B97-D[18] as implemented in the Gaussian09 program.[19] For all main-group elements (C, H, P and Cl) the all-electron triple-ζ basis set (6-311G**) was used.[20] For the transition metals, a

small-core relativistic ECP together with the corresponding double-ζ valence basis set (Stuttgart RSC 1997 ECP) was employed for Fe[21] and Pd,[22] and a small-core relativistic pseudopotential Stuttgart-Köln MCDHF RSC ECP for Hg[23].[24] Natural bond orbital (NBO) calculations were carried out using NBO (Version 3.1),[25] which is part of the Gaussian09 program package. The AIM analyses were performed with the AIMII professional program applying wavefunctions obtained for the optimized structure.[26]

Synthesis of Bis((*ortho*-diphenylphosphino)ferrocenyl)mercury ligands 4a (*meso*-isomer), and 4b (p*S*p*S*/*rac*-isomer). To a solution of *rac*-**2** (0.51 g, 1.00 mmol) in THF (50 mL) that was cooled to −78 °C was added slowly a solution of *t*BuLi in pentane (1.7 M, 0.65 mL, 1.1 mmol, 1.1 equiv). The mixture was stirred for 10 min and a solution of $HgCl_2$ (0.12 g, 0.44 mmol, 0.44 equiv) in THF (10 mL) was slowly added. After stirring for at least 1 hour at this temperature, the reaction mixture was allowed to slowly warm up to room temperature and stirring was continued overnight. The mixture was then filtered to remove insoluble material and the solvent removed in vacuum to leave an orange residue. The latter was purified by flash chromatography on silica gel with hexanes/Et_2O (6:1) as the eluent. The second band was collected, the solvent evaporated, and the residue recrystallized from hexanes at −27 °C to give a yellow crystalline solid. NMR data revealed that the crystals consist of a mixture of two distinct isomers (*meso*-**4a** and *rac*-**4b**, ratio 44:56). Yield 0.19 g (46% for both isomers). High-resolution MALDI-TOF MS (positive mode, anthracene) of the diastereoisomer mixture: m/z 940.0733 (M^+, 100%, calcd for $^{12}C_{44}{}^{1}H_{36}{}^{56}Fe_2{}^{200}Hg^{31}P_2$ 940.0703). The two isomers were preparatively separated by repeated recrystallization from hot hexanes. **4a** (*meso*) crystallized first (0.080 g, 19%) and *rac*-**4b** was subsequently isolated from the mother liquor as a yellow crystalline solid (0.090 g, 22%). A similar route was used for the synthesis of enantiomerically pure (p*S*p*S*)-**4b** starting from a solution of

p*S*-**2** (1.51 g, 2.97 mmol) in THF (40 mL) cooled to −78 °C, to which *t*BuLi (1.7M, 1.7 mL, 2.9 mmol, 1.0 equiv) in pentane was slowly added. After 10 min stirring, the mixture was treated with a solution of $HgCl_2$ (0.39 g, 1.44 mmol, 0.48 equiv) in THF (10 mL). The reaction was worked up as described above and the enantiomerically pure (p*S*p*S*)-**4b** was isolated as an orange crystalline solid. Yield: 0.54 g (40%). Single crystals of **4a** (*meso*) and (p*S*p*S*)-**4b** were obtained from DCM solution layered with hexanes.

For **4a** (*meso*): ^{1}H NMR (599.7 MHz, $CDCl_3$, 25 °C): δ = 7.49 (m, 4H, Ph), 7.37 (m, 6H, Ph), 7.24 (m, 10H, Ph), 4.51 (pt, $^{3}J_{H,H}$ = 1.8 Hz, 2H, Cp), 4.26 (nr, 2H, Cp), 4.13 (nr, 2H, Cp), 4.03 (s, 10H, free Cp). ^{13}C{^{1}H} NMR (150.8 MHz, $CDCl_3$, 25 °C): δ = 141.2 (d, $^{1}J_{C,P}$ = 10.4 Hz, *i*-Ph), 138.3 (d, $^{1}J_{C,P}$ = 9.3 Hz, *i*-Ph), 135.0 (d, $^{2}J_{C,P}$ = 20.8 Hz, *o*-Ph), 132.8 (d, $^{2}J_{C,P}$ = 18.5 Hz, *o*-Ph), 129.2 (s, *p*-Ph), 128.6 (br d, *m*-Ph), 128.4 (d, $^{3}J_{C,P}$ = 6.0 Hz, *m*-Ph), 128.2 (s, *p*-Ph), 110.1 (d, $^{2}J_{C,P}$ = 46.4 Hz, *i*-Cp-Hg), 84.2 (d, $^{1}J_{C,P}$ = 3.5 Hz, *i*-Cp-P), 78.3 (d, $^{2}J_{C,P}$ = 13.9 Hz, Cp), 74.3 (nr, Cp), 73.4 (nr, Cp), 69.1 (s, free Cp). ^{31}P{^{1}H} NMR (202.5 MHz, $CDCl_3$, 25 °C): δ = −13.1 (s). High-resolution ESI-MS (positive mode, CH_2Cl_2/acetonitrile): m/z 940.0683 ([M]$^{+}$, 50%, calcd for $^{12}C_{44}{}^{1}H_{36}{}^{56}Fe_2{}^{200}Hg{}^{31}P_2$ 940.0703). Elem. Anal. for $C_{44}H_{36}Fe_2HgP_2$: Calcd C 56.28, H 3.86; Found C 56.06, H 3.68. For **4b** (*rac*/p*S*p*S*): ^{1}H NMR (599.7 MHz, $CDCl_3$, 25 °C): δ = 7.61 (m, 4H, Ph), 7.39 (m, 6H, Ph), 7.25 (m, 10H, Ph), 4.51 (pt, $^{3}J_{H,H}$ = 1.8 Hz, 2H, Cp), 4.20 (nr, 2H, Cp), 4.15 (nr, 2H, Cp), 4.13 (s, 10H, free Cp). ^{13}C{^{1}H} NMR (150.8 MHz, $CDCl_3$, 25 °C): δ = 141.6 (d, $^{1}J_{C,P}$ = 10.6 Hz, *i*-Ph), 138.4 (d, $^{1}J_{C,P}$ = 9.4 Hz, *i*-Ph), 135.1 (d, $^{2}J_{C,P}$ = 20.8 Hz, *o*-Ph), 132.7 (d, $^{2}J_{C,P}$ = 17.5 Hz, *o*-Ph), 129.3 (s, *p*-Ph), 128.5 (br s, *m*-Ph), 128.1 (s, *p*-Ph), 110.1 (d, $^{2}J_{C,P}$ = 51.0 Hz, *i*-Cp-Hg), 84.4 (nr, *i*-Cp-P), 78.3 (d, $^{2}J_{C,P}$ = 13.9 Hz, Cp), 74.1 (nr, Cp), 73.5 (nr, Cp), 69.3 (s, free Cp). ^{31}P{^{1}H} NMR (202.5 MHz, $CDCl_3$, 25 °C): δ = −13.4 (s). ^{1}H, ^{13}C and ^{31}P-NMR characterization of **4b** (p*S*p*S*) is consistent with reported data for a different synthetic route.[13]

Synthesis of Bis(*ortho*-diphenylphosphinoferrocenyl)mercury Palladium(II) Complex 5a (*meso*). To a solution of dichloro(cyclooctadiene)palladium(II) ($PdCl_2$(COD), 4.1 mg, 0.014 mmol) in anhydrous CH_2Cl_2 (2 mL) was added slowly a solution of *meso*-**4** (13.4 mg, 0.014 mmol) in anhydrous CH_2Cl_2 (2 mL) at room temperature. The color changed immediately from yellow to orange-red. The mixture was stirred for 20 min and the solvent evaporated under reduced pressure. A ^{31}P NMR spectrum of the crude product showed full conversion to a new species. The residue was washed several times with hexanes, collected by filtration and dried under vacuum. Further purification was achieved by column chromatography over a small plug of silica gel with CH_2Cl_2/pentane (1:1) as eluent. Subsequent recrystallization by slow partial evaporation of a solution of the compound in CH_2Cl_2/octane afforded pure **5a** as a red crystalline solid. Yield: 13.0 mg, 81%). Red colored single crystals for X-ray analysis were obtained by slow evaporation of a solution in CH_2Cl_2/hexanes. ^{1}H NMR (599.7 MHz, $CDCl_3$, 25 °C): δ = 8.47 (m, 4H, *o*-Ph), 7.61 (m, 6H, *m,p*-Ph), 7.11 (t, ^3J = 7.5 Hz, 2H, *p*-Ph'), 7.06 (pt, ^3J = 7.5 Hz, 4H, *m*-Ph'), 6.82 (m, 4H, *o*-Ph'), 4.69 (pt, $^3J_{H,H}$ = 2.4 Hz, 2H, Cp), 4.61 (br d, 2H, Cp), 4.59 (br d, 2H, Cp), 4.12 (s, 10H, free Cp). ^{13}C{^{1}H} NMR (150.8 MHz, $CDCl_3$, 25 °C): δ = 136.3 (pt, $^{2,4}J_{C,P}$ = 5.3 Hz, *o*-Ph), 136.3 (pt, $^{1,3}J_{C,P}$ = 26 Hz, *i*-Ph), 133.1 (pt, $^{2,4}J_{C,P}$ = 5.3 Hz, *o*-Ph'), 132.4 (pt, $^{1,3}J_{C,P}$ = 26 Hz, *i*-Ph'), 131.3 (s, *p*-Ph), 129.2 (s, *p*-Ph'), 128.2 (pt, $^{3,5}J_{C,P}$ = 5.3 Hz, *m*-Ph), 127.2 (pt, $^{3,5}J_{C,P}$ = 5.3 Hz, *m*-Ph'), 113.1 (pt, $^{2,4}J_{C,P}$ = 19 Hz, *i*-Cp-Hg), 81.0 (pt, $^{1,3}J_{C,P}$ = 30 Hz, *i*-Cp-P), 77.6 (overlapped, Cp), 75.9 (pt, $^{3,5}J_{C,P}$ = 3.1 Hz, Cp), 74.0 (br s, Cp), 70.7 (s, free Cp). ^{31}P{^{1}H} NMR (202.5 MHz, $CDCl_3$, 25 °C): δ = 23.6 (s). High-resolution ESI-MS (positive mode, CH_2Cl_2/acetonitrile): m/z 1080.9438 ($[M-Cl]^+$, 100%, calcd for $^{12}C_{44}{}^1H_{36}{}^{35}Cl^{56}Fe_2{}^{200}Hg^{31}P_2{}^{106}Pd$ 1080.9421).

Synthesis of Bis(*ortho*-diphenylphosphinoferrocenyl)mercury palladium(II) complexes 5b (p*S*p*S*). The isomer **5b** was obtained using a similar procedure as for **5a**. To a solution of **4b** (13.4

mg, 0.014 mmol) in anhydrous CH_2Cl_2 (2 mL) was added slowly a solution of dichloro(cyclooctadiene)palladium(II), $PdCl_2$(COD), (4.1 mg, 0.014 mmol) in anhydrous CH_2Cl_2 (2 mL) at room temperature. The color changed immediately from yellow to orange-red. The mixture was stirred for 20 min under N_2 atmosphere and then passed through a small plug of silica gel. All volatiles were removed under high vacuum and the residue was washed several times with hexanes to yield a light orange solid. Yield: 11.9 mg, 75%. Red colored single crystals for X-ray analysis were obtained from a solution in toluene/hexanes at –27 °C. ^{1}H NMR (599.7 MHz, $CDCl_3$, 25 °C): δ = 8.28 (m, 4H, *o*-Ph), 7.44 (t, 2H, ^3J = 7.2 Hz *p*-Ph), 7.41 (m, 4H, *m*-Ph), 7.28 (t, ^3J = 7.2 Hz, 2H, *p*-Ph'), 7.24 (m, 4H, *m*-Ph'), 7.10 (m, 4H, *o*-Ph'), 4.75 (pt, $^3J_{H,H}$ = 2.4 Hz, 2H, Cp), 4.64 (br d, 2H, Cp), 4.56 (br d, 2H, Cp), 4.10 (s, 10H, free Cp). ^{13}C{^{1}H} NMR (150.8 MHz, $CDCl_3$, 25 °C): δ = 136.0 (pt, $^{2,4}J_{C,P}$ = 6.6 Hz, *o*-Ph), 135.9 (pt, $^{1,3}J_{C,P}$ = 26 Hz, *i*-Ph), 133.4 (pt, $^{2,4}J_{C,P}$ = 5.3 Hz, *o*-Ph'), 132.7 (pt, $^{1,3}J_{C,P}$ = 26 Hz, *i*-Ph'), 130.8 (s, *p*-Ph), 129.4 (s, *p*-Ph'), 128.0 (pt, $^{3,5}J_{C,P}$ = 5.7 Hz, *m*-Ph), 127.4 (pt, $^{3,5}J_{C,P}$ = 5.2 Hz, *m*-Ph'), 111.0 (pt, $^{2,4}J_{C,P}$ = 18 Hz, *i*-Cp-Hg), 79.7 (pt, $^{1,3}J_{C,P}$ = 29 Hz, *i*-Cp-P), 78.1 (pt, $^{2,4}J_{C,P}$ = 8.4 Hz, Cp), 75.8 (pt, $^{3,5}J_{C,P}$ = 3.1 Hz, Cp), 74.3 (br s, Cp), 70.6 (s, free Cp). ^{31}P{^{1}H} NMR (202.5 MHz, $CDCl_3$, 25 °C): δ = 20.3 (s). High-resolution ESI-MS (positive mode, CH_2Cl_2/acetonitrile): 1080.9437 ([M–Cl]$^+$, 100%, calcd for $^{12}C_{44}{}^1H_{36}{}^{35}Cl^{56}Fe_2{}^{200}Hg^{31}P_2{}^{106}Pd$ 1080.9421). Elem. Anal. for $C_{44}H_{36}Cl_2Fe_2HgP_2Pd$: Calcd C 47.34, H 3.25; Found C 47.43, H 3.07.

Competition reaction of 4a/4b with $PdCl_2$(COD). A solution containing **4a** (0.010 g, 0.011 mmol) and **4b** (0.010 g, 0.011 mmol) in $CDCl_3$ (0.7 mL) was added slowly to a solution of $PdCl_2$(COD) (0.0031 g, 0.011 mmol) in $CDCl_3$ (0.3 mL) at room temperature. The mixture was introduced into an NMR tube and the reaction followed by ^{31}P NMR spectroscopy. After 0.5 h standing at room temperature: ^{31}P{^{1}H} NMR (202.5 MHz, $CDCl_3$, 25 °C): δ = −13.4 (18%), −13.7

(20%), 21.2 (26%), 23.0 (36%). After overnight standing at room temperature: $^{31}P\{^{1}H\}$ NMR (202.5 MHz, $CDCl_3$, 25 °C): δ = −13.4 (17%), −13.7 (20%), 21.2 (28%), 23.0 (36%).

Results and Discussion

Synthesis of Isomeric Diphosphine Ligands 4a and 4b. To prepare the diferrocenylmercury-bridged bis(diphenylphosphine)s **4a** (*meso*-isomer) and **4b** (p*S*p*S*-/*rac*-isomer), we adopted a salt metathesis procedure similar to that previously reported for the synthesis of **DPHg**[27] (Chart 1) and related[28] chelate ligands. As illustrated in Scheme 1, the independent preparation of **4a** and **4b** requires racemic and single enantiomer (*ortho*-diphenylphosphino)ferrocenyl sulfinate (*rac*-**2** and p*S*-**2**) as starting materials, respectively, which in turn are readily obtained from ferrocenylsulfinate **1** according to published procedures.[15] Thus, *rac*-**2** was treated with 1.1 equivs of *t*-BuLi in THF at –78 °C followed by *in-situ* reaction of the resulting *ortho*-lithiated diphenylphosphinoferrocene (**3**) with 0.44 equivs of $HgCl_2$. Upon flash column chromatography with hexanes/Et_2O (6:1), a mixture of the bidentate ambiphilic ligands *meso*-/rac-**4** was isolated as a yellow-orange solid in 46% yield. The ^{31}P NMR spectrum showed two closely spaced resonances at δ = –13.1 and –13.4 ppm in an integral ratio of 44:56 (*meso*:*rac*) and the ^{1}H NMR spectrum displayed two sets of signals, suggesting the formation of the two diastereomers in an approximate 1:1 ratio. Consistent with the formation of a mixture of isomers, high resolution MALDI-TOF MS analysis revealed only a single mass cluster at m/z = 940.0661 corresponding to $[\mathbf{4}]^+$. Attempts to separate **4a** (*meso*) from the diastereomer mixture by column chromatography were unsuccessful. Fortunately, repeated recrystallization from hot hexanes resulted in the separation and full characterization of **4a**, which crystallizes first in the form of parallelepiped crystals in 19% yield. The racemate **4b** was subsequently isolated from the mother liquor in the form of block-shaped

crystals in 22% isolated yield. Single crystal X-ray diffraction analyses (*vide infra*) confirmed that the parallelepiped crystals correspond to **4a** ($\delta(^{31}P) = -13.1$, $\delta(^{1}H) = 4.03$ (free Cp), 4.13, 4.26, 4.51 (substituted Cp)) and the block-shaped crystals to *rac*-**4b** ($\delta(^{31}P) = -13.4$ ppm, $\delta(^{1}H) = 4.13$ (free Cp), 4.15, 4.20, 4.51 ppm (substituted Cp)). ESI-MS analyses further confirmed the formation of **4a** and **4b**. A similar route was applied for the synthesis of enantiomerically pure **4b** from (p*S*p*S*)-**2** and the compound obtained in 40% isolated yield as an orange crystalline solid after recrystallization from hexanes at −25 °C. As expected, the ^{31}P NMR spectrum exhibited a resonance at $\delta = -13.4$ ppm, which is at essentially the same chemical shift as for racemic **4b**. In addition, the chirality of (p*S*p*S*)-**4b** was established by optical rotation measurements in chloroform, which yielded a specific rotation of $[\alpha]^{20}_{D} = +250$ (*c* 0.1). Both **4a** and **4b** are readily soluble in organic solvents; they are stable toward air and moisture, but when kept in solution under air for a long period of time, gradual oxidation of P occurs as indicated by the appearance of new signals at lower field in the ^{31}P NMR spectrum.

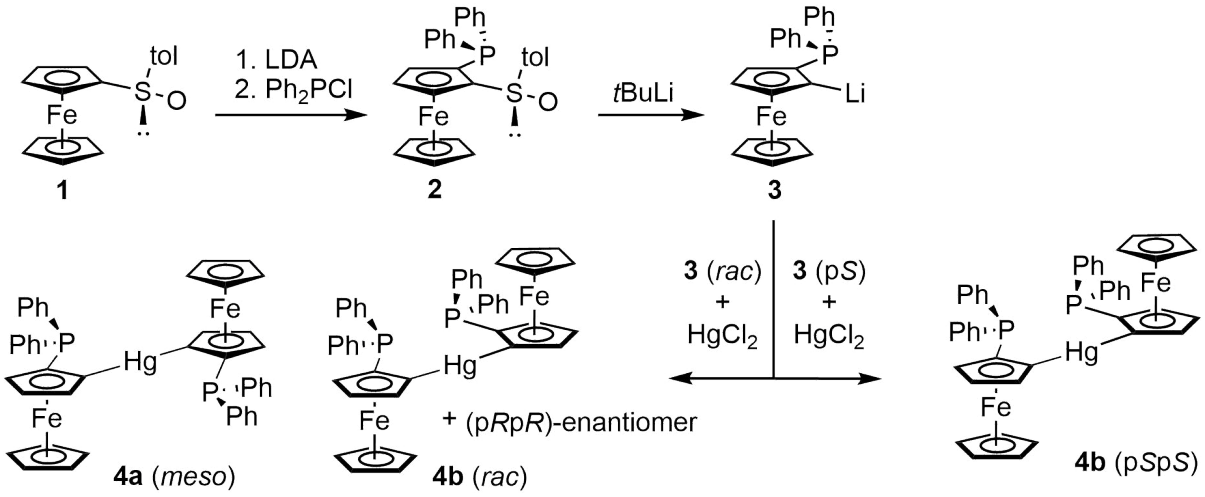

Scheme 1. Synthesis of the ambiphilic diphosphine ligands *meso*-**4a**, *rac*-**4b** and (p*S*p*S*)-**4b**.

The main difference between the structures of **4a** ($P2_1/n$) and racemic **4b** (P–1) lies in the orientation of the ferrocene moieties relative to the central Hg atom (Figure 1). The centrosymmetric *meso*-isomer **4a** adopts a *trans* conformation where the ferrocene moieties are on opposite sides of the central Cp-Hg-Cp fragment, which also results in a *trans* arrangement of the phosphine ligands with respect to the Hg atom. For the corresponding *rac*-isomer **4b**, a similar *trans* orientation of the ferrocene moieties would place the PPh_2 moieties in too close proximity to one another. Avoiding steric congestion, **4b** adopts a twisted orientation with an interplanar angle between the substituted Cp rings of 57.5° and a P1···Hg···P2 angle of 134.2(1)°. In addition, while the Hg atom adopts a perfectly linear geometry in **4a** (C1–Hg–C1A = 180°), a modest distortion is evident for **4b** (C1–Hg–C23 = 174.67(14)°). The Hg···P distances of 3.5744(8) Å in **4a** are slightly shorter than those found for **4b** (3.5968(11), 3.6148(10) Å) and, in both cases, they are at just about the sum of the van der Waals radii for P (1.80)[29] and Hg (2.05 Å)[30], demonstrating that secondary interactions are relatively weak or absent. This is in contrast to the much shorter P→Hg contacts reported for **DPHg** (3.001(2) and 2.973(2) Å).[28]

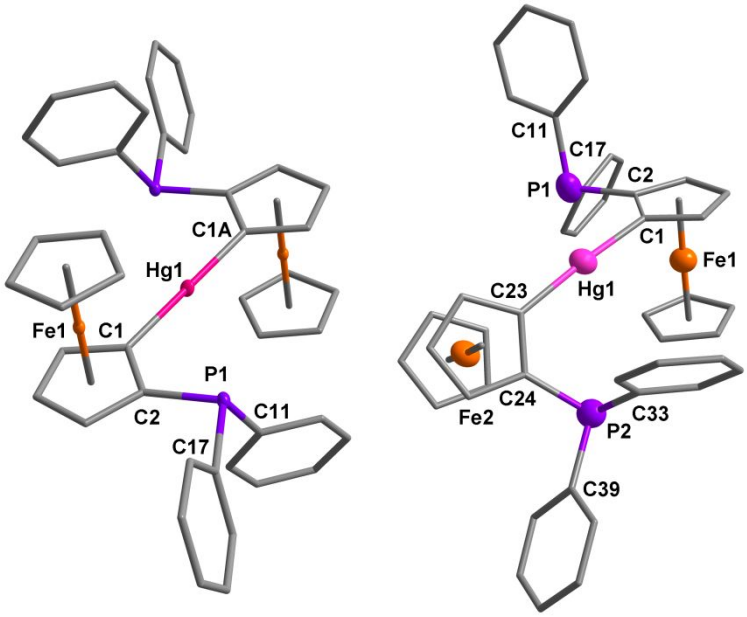

Figure 1. Molecular structures of *meso*-**4a** (left) and *rac*-**4b** (right) (50% thermal ellipsoids, hydrogen atoms omitted for clarity). Selected interatomic distances (Å) and angles (°) for *meso*-**4a**: P1-C2 1.820(3), Hg1−C1 2.053(3), Hg1···P1 3.5744(8), C1−Hg1−C1A 180, dihedral angle for substituted Cp//Cp 0; *rac*-**4b**: P1-C2 1.812(4), P2-C24 1.819(4), Hg1−C1 2.068(4), Hg1−C23 2.070(5), Hg1···P1 3.5968(11), Hg1···P2 3.6148(10), C1−Hg1−C23 174.67(14), dihedral angle for substituted Cp//Cp 57.5.

Having the ambiphilic diphosphine ligands **4a** and **4b** in hand, we sought to explore their coordination toward transition metals. The bite angle of diphosphine ligands is known to have a pronounced effect on the reactivity and selectivity of transition metal catalysts.[2a, 3, 31] The new ligands **4** should offer not only access to unusually wide bite angles but also display a high degree of variability of the bite angle. Indeed, the observation of a single set of ^{1}H NMR resonances indicates free rotation about the Cp-Hg-Cp axis in solution and, thus, the ligands are expected to readily adopt the most suitable conformation for metal coordination. They are unique also in that the 3-dimensional structure of the ferrocene moieties offers a spatial environment not encountered for any other ligand class. Moreover, a dramatically different environment is expected for **4a** versus **4b**. Finally, the presence of the Lewis acidic mercury atom as a bridging element between the phosphine binding sites may lead to rare and interesting secondary M···Hg metallophilic interactions.

Complexation to Pd(II) and Structural Characterization. Upon independently mixing the diphosphine isomers **4a** and **4b**, each with one equivalent of $PdCl_2$(COD), the color of the solutions rapidly changed from yellow to orange-red with formation of the palladium(II) complexes **5a** and **5b** in 81% and 75% yield respectively (Scheme 2). A similar procedure also provided (p*S*,p*S*)-**5b** ($[\alpha]^{20}_{D} = -70$ in $CHCl_3$) when starting from (p*S*,p*S*)-**4b**. Coordination of the phosphorus atoms to

palladium manifests itself in the ^{31}P NMR spectra with resonances for **5a** and **5b** at δ = 23.6 and 20.3 ppm, respectively, that are shifted by $\Delta\delta$ = 36.7 and 33.7 ppm in comparison to those of **4a** and **4b**. The ^{1}H NMR spectra of the palladium complexes are markedly different from those of the free ligands as exemplified by a distinct downfield shift of the protons on the substituted Cp rings from δ = 4.13, 4.26, 4.51 ppm to δ = 4.59, 4.61, 4.69 ppm for **5a**, and from δ = 4.15, 4.20, 4.51 ppm to δ = 4.56, 4.64, 4.75 ppm for **5b**. The phenyl groups are non-equivalent and one set of signals (δ = 8.48 ppm for *ortho*-protons of **5a**; δ = 8.28 ppm for *ortho*-protons of **5b**) is shifted to lower field and is thus less effectively shielded than the other. The formation of the Pd(II) complexes **5a** and **5b** is further evidenced by high resolution ESI-MS analysis, which shows mass clusters at m/z = 1080.9438 and 1080.9437 a. u. assigned to [**5a**−Cl]$^{+}$ and [**5b**−Cl]$^{+}$, respectively.

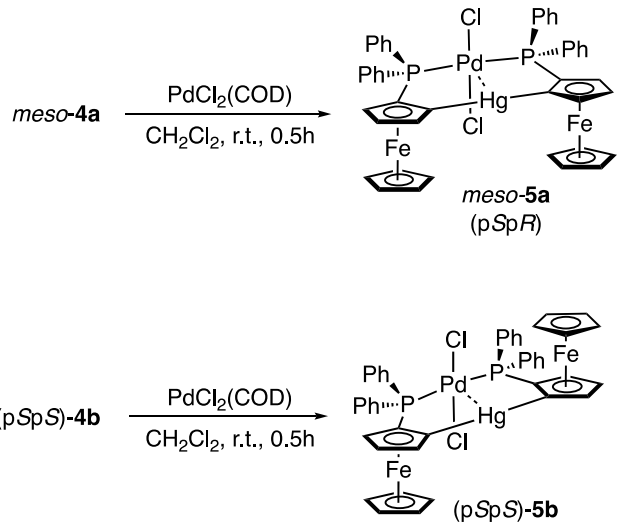

Scheme 2. Synthesis of Pd(II) complexes **5a** and **5b**.

To evaluate any differences in reactivity between isomers **4a** and **4b** toward $PdCl_2$(COD), competitive reactions were performed using an approximately equimolar mixture of each of the isomers and the respective palladium precursor. The ^{31}P NMR spectrum (Figure S1, SI) of a sample

containing a mixture of **4a**, **4b**, and $PdCl_2$(COD) in a molar ratio of ca. 1:1:1 showed after 30 min the expected product signals at δ = 23.0 (36%, **5a**) and 21.2 (26%, **5b**), together with resonances of the free ligands at δ = −13.4 (18%, **4a**) and −13.7 (20%, **4b**). Further reaction for another 24 h did not induce significant changes to the signal intensities. We conclude that the chelate ligands **4a** and **4b** show relatively similar reactivity in the formation of palladium(II) complexes with $PdCl_2$(COD), with a slight preference for reaction with **4a**. The preferential reactivity of **4a** over **4b** suggests a lower kinetic barrier for the binding of $PdCl_2$ for **4a**. Looking at the differences in the X-ray structures of **5a** and **5b** (*vide infra*), a possible explanation is that in the formation of **5a** the $PdCl_2$ moiety can approach from above the diferrocenyl mercury framework, avoiding interference with the ferrocenyl groups.

Red colored single crystals of **5a** appropriate for X-ray diffraction analysis were obtained by slow evaporation of a CH_2Cl_2/hexanes solution at room temperature and crystals of (p*S*,p*S*)-**5b** were grown from a toluene/hexanes solution at –27 ºC. The molecular structures of **5a**·CH_2Cl_2 and (p*S*,p*S*)-**5b**·toluene (Figure 2) show the Hg in an almost linear environment (C1–Hg1–C23 = 177.6(3), 175.2(5) Å) and the phosphino groups are positioned *cis* with respect to the Fc_2Hg moiety, in contrast to the orientation of the free ligands. For both structures an unusual *trans* chelation of the square-planar Pd(II) atom is evident with P1–Pd1–P2 angles of 174.32(7)º and 175.49(7)° that are very close to the ideal angle of 180º. A survey of M(II)Cl_2L_2 (M = Pd, Pt) complexes of common phosphine ligands shows that this bite angle is the highest ever reported for diphosphine chelate ligands (Table 1). The bite angles in **5a** and (p*S*,p*S*)-**5b** are also higher than that in the phenylene analogue [$PdCl_2${Hg(*o*-$C_6H_4PPh_2$)}] (168.45(9)º).[27b]

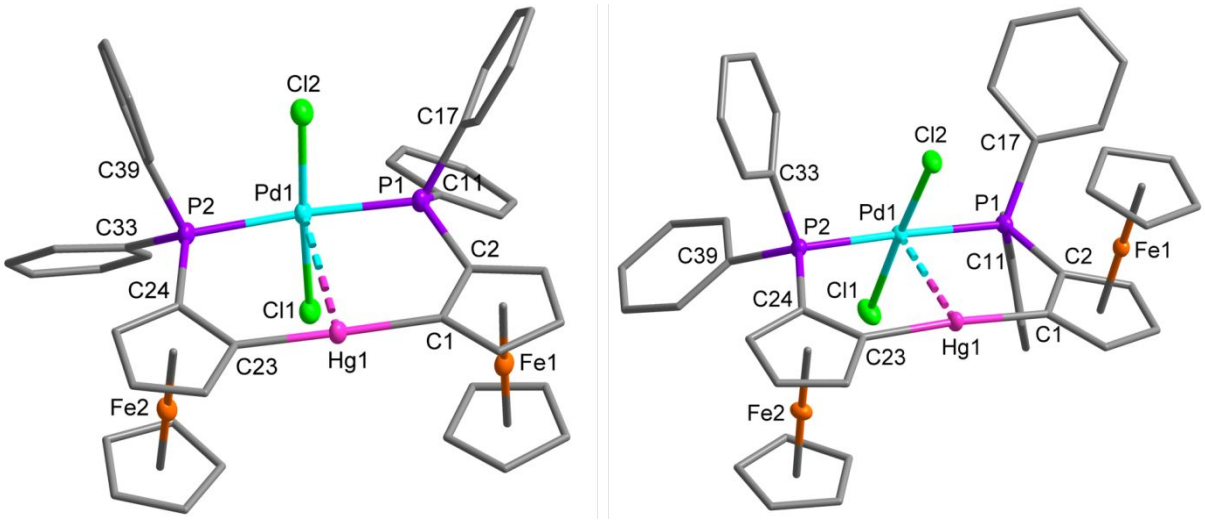

Figure 2. Molecular structures of **5a**·CH_2Cl_2 (left) and (p*S*,p*S*)-**5b**·toluene (right) (50% thermal ellipsoids, H atoms and solvent molecule omitted for clarity). Selected interatomic distances (Å) and angles (°) for *meso*-**5a**: Pd1–P1 2.3272(19), Pd1–P2 2.3654(19), Pd1–Cl1 2.313(2), Pd1–Cl2 2.270(2), Pd1···Hg1 2.9828(6), P1–C2 1.817(7), P2–C24 1.801(7), Hg1−C1 2.077(7), Hg1–C23 2.072(7), C1−Hg1−C23 177.6(3), P1–Pd−P2 174.32(7), Cl1–Pd1–Cl2 175.38(7), dihedral angle for substituted Cp//Cp 4.9; for (p*S*,p*S*)-**5b**: Pd1–P1 2.347(2), Pd1–P2 2.344(2), Pd1–Cl1 2.299(2), Pd1–Cl2 2.304(2), Pd1···Hg1 2.9313(10), P1–C2 1.817(10), P2–C24 1.790(11), Hg1−C1 2.080(7), Hg1–C23 2.087(7), C1−Hg1−C23 175.2(3), P1–Pd−P2 175.49(7), Cl1–Pd1–Cl2 176.19(8), dihedral angle for substituted Cp//Cp 11.5.

Table 1. Comparison of bite angles for complexes **5** with those of other common Pd(II) and Pt(II) diphosphine chelate complexes.

Diphosphine Complex[a]	**Bite angle (°)**	**Diphosphine Complex**[a]	**Bite angle (°)**
5a	174.2	(DPEphos)$PdCl_2$[31a]	102.9
(p*S*,p*S*)-**5b**	175.5	(Xantphos)$PdCl_2$[3, 31a]	110.0
(dppe)$PdCl_2$[32]	85.82(7)	(SPANphos)$PtCl_2$[4]	171.9
(dppf)$PdCl_2$[32b]	99.07(5)	(PhTrap)$PdBr_2$[11a]	163.6(1)

[a] dppe = 1,2-bis(diphenylphosphino)ethane, dppf = 1,1'-bis(diphenylphosphino)ferrocene, DPEphos = bis[(2-diphenylphosphino)phenyl]ether, Xantphos = 4,5-bis(diphenylphosphino)-9,9-dimethylxanthene, PhTrap = (*S*,*S*)-(R,R)-2,2''-bis[1-(diphenylphosphino)-ethyl]-1,1''-

biferrocene, SPANphos = (*rac*)-8,8'-bis(diphenylphosphino)-3,3',4,4'-tetrahydro-4,4,4',4',6,6'-hexamethyl-2,2'-spirobi[2H-1-benzopyran].

A major difference between the two Pd complexes is that, due to the different stereochemistry, the ferrocene moieties are adjacent to one another in the *meso*-complex, but they are placed on opposite sides in (p*S*,p*S*)-**5b** with respect to the plane defined by the substituted Cp rings, the P atoms, Hg and Pd (see Figure S2a for a 3D-illustration). The eight atoms involved in the central C_4HgPdP_2 heterocycle form an almost planar structure in **5a** marked by a very small twist between the substituted Cp rings of only 4.9º; the latter is significantly larger in (p*S*,p*S*)-**5b** at 11.5º due to steric interference of the PPh_2 groups and the Cl atoms on Pd. The relative position of the ferrocene moieties also has a pronounced effect on the orientation of the $PdCl_2$ fragment relative to the Fc_2Hg moiety. For **5a** the Cl1-Pd-Cl2 vector is tilted towards the ferrocene moieties as evidenced by a small Hg1···Pd1-Cl1 angle of 71.77(5)º and large Hg1···Pd1-Cl2 angle of 111.22(5)º. For (p*S*,p*S*)-**5b**, a much more modest tilting of Cl2 towards one of the ferrocenes and Cl1 away from the other ferrocene is observed and, consequently, the respective angles of 99.39(6)º and 76.80(6)º are much closer to 90º. As a result, for **5a** the Cl1 chlorine atom appears to be bridging the two unsubstituted Cp rings of the ferrocenes (Cl1···H30 2.844(2), Cl1···H7 3.008(2) Å) and also shows a short contact to one of the phenyl rings on phosphorous (Cl1···H34 2.711(2) Å), whereas for **5b** both Cl1 and Cl2 are in close proximity to only one of the unsubstituted Cp rings (Cl1···H29 2.876(2) Å; Cl2···H7 2.998(2); Figure S2b). Possibly also related is the observation that the Pd-Cl distances for *meso*-**5a** (2.270(2), 2.313(2) Å) are more dissimilar than those for (p*S*,p*S*)-**5b** (2.299(2), 2.304(2) Å), with the longest Pd-Cl distance observed for the chlorine atom that is acting as a bridging hydrogen bond acceptor in **5a**. The Pd atoms also show short contacts to Hg of 2.9828(6) Å for *meso*-**5** and 2.9313(10) Å for (p*S*,p*S*)-**5b**, at a distance that is only slightly longer than the

value of 2.8797(8) Å measured for $[PdCl_2\{Hg(o\text{-}C_6H_4PPh_2)\}]$[27b]. This offers a strong indication of an intramolecular Pd···Hg metallophilic interaction with the diorganomercury moiety, considering also that the distance is well below those of related compounds[33] for which Pd···Hg interactions have previously been claimed [3.1020(3)–3.2841(2) Å].

Computational Investigation of Pd(II)···Hg(II) Metallophilic Interactions. The possibility of metallophilic Pd···Hg interactions in the two isomers *meso*-**5a** and (p*S*p*S*)-**5b** was further examined by computational methods. The calculations were performed using the hybrid density functional B97-D with a 6-311g** basis set for C, H, Cl and P, a Stuttgart RSC 1997 ECP basis set for Fe and Pd, and a Stuttgart-Koeln MCDHF RSC ECP basis set for Hg. The interatomic Pd···Hg distances of the optimized structures (2.9775 Å for optimized **5a**, 2.9721 Å for optimized **5b**; Figure S3) are very close to the experimental values from the X-ray structures (2.9828(6) Å for **5a**, 2.9313(10) Å for **5b**). An evaluation of the total energies (at 0 and 298K) of the optimized isomers revealed a slightly lower energy for **5b** in comparison to **5a** (ΔE = 1.2 and 1.3 kcal mol^{-1}), suggesting that the **5b**-isomer is thermodynamically favoured (even though **5a** formed preferentially in the competition experiment). Wiberg bond indices (WBIs) of 0.15 (**5a**) and 0.16 (**5b**) were calculated for the Pd···Hg interactions, which are in the same range as that (WBI = 0.12) of a previously reported complex[33d] for which a Pd···Hg metallophilic interaction had been postulated. Atom in Molecules (AIM) analysis of the geometry-optimized molecules revealed bond paths between the Hg and the Pd atom with similar electron densities of $\rho(r) = 2.9 \times 10^{-2}$ e/a_0^3 and Laplacians of the electron density (7.2×10^{-2} e/a_0^5) for both isomers at the Pd···Hg bond critical points (BCPs) (Figure 3). The electron densities at the BCPs are relatively larger and should therefore likely reflect stronger interactions than those reported previously for complexes[33c, 33d] with Pd···Hg interactions (1.0×10^{-2}, 1.3×10^{-2}, and 1.7×10^{-2} e/a_0^3). However, an analysis of the

relevant molecular orbitals shows that, although binding σ-MOs can be observed, any contribution to a Pd-Hg bond is minimal since the associated antibonding σ*-MOs are also doubly occupied (Figure S5). Weak hydrogen bonding interactions were observed in the optimized structures (Figure S3), similar to those detected in the single crystal X-ray structure analyses (Figure S2), and further confirmed by the presence of bond paths and bond critical points between the chlorine and the Cp or Ph ring hydrogen atoms. AIM contour plots of the relevant contacts are presented in Figure S4.

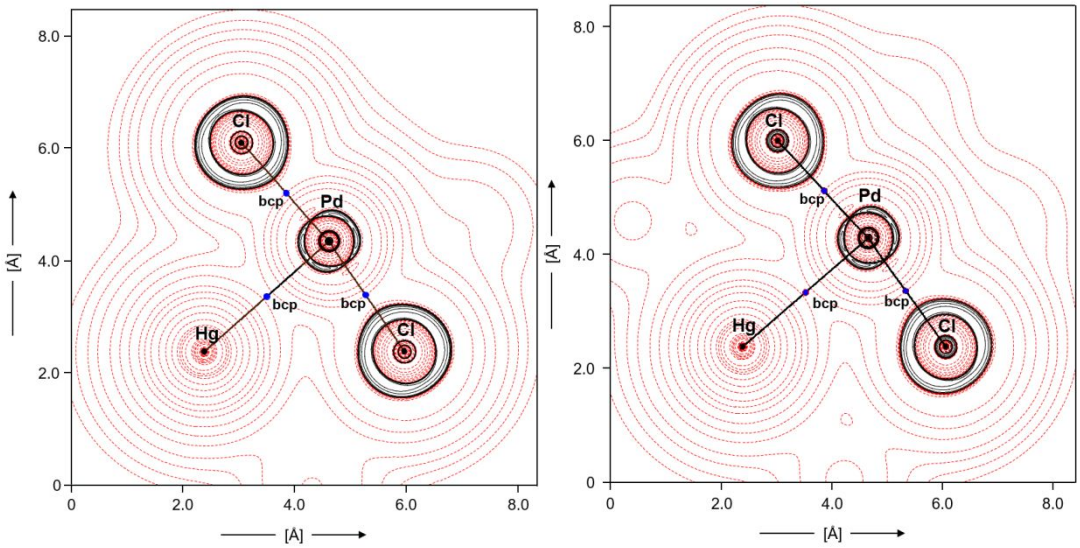

Figure 3. AIM contour plot of the Laplacian for *meso*-**5a** (left) *and* (p*S*p*S*)-**5b** (right) showing the bond paths (black line) and the bond critical points (BCPs as blue circle) between Pd and Hg.

Conclusions

A new class of ferrocene-based ambiphilic chelate ligands with a unique 3-dimensional structure was generated by salt metathesis of *ortho*-lithiated diphenylphosphinoferrocene with $HgCl_2$. Single crystal X-ray analyses revealed a *trans* arrangement of the ferrocene moieties in the solid-state structure of the *meso*-isomer **4a**, but a more twisted conformation for the *rac*-isomer **4b**. The

latter avoids steric congestion due to the close proximity of the diphenylphosphino moieties in a *cis*-arrangement. The coordination of these diphosphine ligands to Pd(II) was investigated, revealing exceptionally large bite angles (β = 174.2 – 175.5°). The flexibility of the bite angle is seen by comparison to a previously reported Hg(II) complex with a much smaller value of β = 138.36(5)°. The molecular structures of the *trans*-chelated Pd(II) complexes *meso*-**5a** and (p*S*,p*S*)-**5b** also suggested the presence of Pd···Hg metallophilic interactions, highlighting the ambiphilic properties of the diphosphine ligands. This aspect was further studied by computational methods, with AIM computations revealing bond-critical points with significant electron densities, but analyses of the molecular orbitals suggesting that the interactions are very weak at best. The Hg-bridged diferrocenyldiphosphines discussed in here represent a new type of chelate ligands with unprecedented metal coordination behaviors, holding promise for stereoselective transition metal-catalyzed transformations.

Acknowledgements

A.C.T.K. thanks the Deutsche Forschungsgemeinschaft (DFG) for a postdoctoral fellowship. A 500 MHz NMR spectrometer used in these studies was purchased with support from the NSF-MRI program (1229030). The X-ray diffractometer was purchased with support from the NSF-CRIF program (0443538) and Rutgers University (Academic Excellence Fund).

References

1. J. A. Gillespsie, E. Zuidema, P. W. N. M. Leuwen, P. C. J. Kamer, *Phosphorus Ligand Effects in Homogenous Catalysis and Rational Catalyst Design, in Phosphorus(III) Ligands in Homogeneous Catalysis: Design and Synthesis*, 1st Edition, P. C. J. Kamer and P. W. N. M. Leuwen, eds.; Wiley, 2012.

2. a) P. Dierkes and P. W. N. M. van Leeuwen, *J. Chem. Soc., Dalton Trans.*, 1999, 1519-1529; b) P. W. N. M. van Leeuwen, P. C. J. Kamer, J. N. H. Reek and P. Dierkes, *Chem. Rev.*, 2000, **100**, 2741-2769; c) P. C. J. Kamer, P. W. N. van Leeuwen and J. N. H. Reek, *Acc. Chem. Res.*, 2001, **34**, 895-904; d) W. J. van Zeist, R. Visser and F. M. Bickelhaupt, *Chem. - Eur. J.*, 2009, **15**, 6112-6115.

3. M. Kranenburg, Y. E. M. Vanderburgt, P. C. J. Kamer, P. W. N. M. Vanleeuwen, K. Goubitz and J. Fraanje, *Organometallics*, 1995, **14**, 3081-3089.

4. Z. Freixa, M. S. Beentjes, G. D. Batema, C. B. Dieleman, G. P. F. van Strijdonck, J. N. H. Reek, P. C. J. Kamer, J. Fraanje, K. Goubitz and P. W. N. M. van Leeuwen, *Angew. Chem. Int. Ed.*, 2003, **42**, 1284-1287.

5. For examples of other trans-coordinating ligands, see: a) C. A. Bessel, P. Aggarwal, A. C. Marschilok and K. J. Takeuchi, *Chem. Rev.*, 2001, **101**, 1031-1066; b) C. M. Thomas, R. Mafua, B. Therrien, E. Rusanov, H. Stoeckli-Evans and G. Suss-Fink, *Chem. - Eur. J.*, 2002, **8**, 3343-3352; c) J. I. van der Vlugt, R. Sablong, A. M. Mills, H. Kooijman, A. L. Spek, A. Meetsma and D. Vogt, *Dalton Trans.*, 2003, 4690-4699; d) R. C. Smith, C. R. Bodner, M. J. Earl, N. C. Sears, N. E. Hill, L. M. Bishop, N. Sizemore, D. T. Hehemann, J. J. Bohn and J. D. Protasiewicz, *J. Organomet. Chem.*, 2005, **690**, 477-481; e) R. C. Smith and J. D. Protasiewicz, *Organometallics*, 2004, **23**, 4215-4222; f) N. H. T. Huy, P. Chaigne, I. Dechamps, L. Ricard and F. Mathey, *Heteroatom Chem*, 2005, **16**, 44-48; g) M. R. Eberhard, K. M. Heslop, A. G. Orpen and P. G. Pringle, *Organometallics*, 2005, **24**, 335-337.

6. a) J. A. Buss, D. G. VanderVelde and T. Agapie, *J. Am. Chem. Soc.*, 2018, **140**, 10121-10125; b) J. A. Buss, G. A. Edouard, C. Cheng, J. D. Shi and T. Agapie, *J. Am. Chem. Soc.*, 2014, **136**, 11272-11275; c) K. T. Horak, D. G. VanderVelde and T. Agapie, *Organometallics*, 2015, **34**, 4753-4765; d) A. Velian, S. B. Lin, A. J. M. Miller, M. W. Day and T. Agapie, *J. Am. Chem. Soc.*, 2010, **132**, 6296-6297.

7. (a) F.-G. Fontaine, J. Boudreau, M.-H. Thibault, *Eur. J. Inorg. Chem.* 2008, 5439-5454. (b) H. Kameo and H. Nakazawa, *Chem. Asian J.* 2013, **8**, 1720-1734. (c) S. R. Tamang, J.-H. Son and J. D. Hoefelmeyer, *Dalton Trans.*, 2014, **43**, 7139-7145 (d) B. E. Cowie, D. J. H. Emslie, *Chem. Eur. J*. 2014, **20**, 16899-16912. (c) G. Bouhadi, D. Bourissou, *Chem. Soc. Rev*. 2016, **45**, 1065-1079. (e) F.-G. Fontaine and É. Rochette, *Acc. Chem. Res*. 2018, **51**, 454-464.

8. a) A. Amgoune and D. Bourissou, *Chem. Commun.*, 2011, **47**, 859-871; b) J. S. Jones and F. P. Gabbaï, *Acc. Chem. Res.*, 2016, **49**, 857-867; c) S. Sahu and F. P. Gabbaï, *J. Am. Chem. Soc.*, 2017, **139**, 5035-5038; d) D. You and F. P. Gabbaï, *J. Am. Chem. Soc.*, 2017, **139**, 6843-6846.

9. J. W. Taylor, A. McSkimming, M. E. Moret and W. H. Harman, *Angew. Chem. Int. Ed.*, 2017, **56**, 10413-10417.

10. a) T. J. Colacot, S. Parisel, Synthesis, Coordination Chemistry and Catalytic Use of dppf Analogs. In Ferrocenes: Ligands, Materials and Biomolecules; Štěpnička, P., Ed.; Wiley: West Sussex, England, 2008; pp 117−140; b) B. L. Blass, R. H. Sanchez, V. A. Decker, M. J. Robinson, N. A. Piro, W. S. Kassel, P. L. Diaconescu and C. Nataro, *Organometallics*, 2016, **35**, 462-470; c) K. M. Gramigna, J. V. Oria, C. L. Mandell, M. A. Tiedemann, W. G. Dougherty, N. A. Piro, W. S. Kassel, B. C. Chan, P. L. Diaconescu and C. Nataro, *Organometallics*, 2013, **32**, 5966-5979; d) S. Sadeh, M. P. T. Cao, J. W. Quail, J. F. Zhu and J. Müller, *Chem.-Eur. J.*, 2018, **24**, 8298-8301.

11. a) M. Sawamura, H. Hamashima, M. Sugawara, R. Kuwano and Y. Ito, *Organometallics*, 1995, **14**, 4549-4558; b) R. G. Arrayas, J. Adrio and J. C. Carretero, *Angew. Chem. Int. Ed.*, 2006, **45**, 7674-7715.

12. a) J. Chen, A. C. T. Kuate, R. A. Lalancette and F. Jäkle, *Organometallics*, 2016, **35**, 1964-1972; b) J. W. Chen, D. A. M. Parra, R. A. Lalancette and F. Jäkle, *Angew. Chem. Int. Ed.*, 2015, **54**, 10202-10205; c) J. W. Chen, R. A. Lalancette and F. Jäkle, *Chem. - Eur. J.*, 2014, **20**, 9120-9129; d) J. W. Chen, R. A. Lalancette and F. Jäkle, *Organometallics*, 2013, **32**, 5843-5851.

13. A. C. Tagne Kuate, R. A. Lalancette, T. Bannenberg and F. Jäkle, *Angew. Chem. Int. Ed.*, 2018, **57**, 6552-6557.

14. A. C. Tagne Kuate, R. A. Lalancette and F. Jäkle, *Organometallics*, 2019, **38**, 677-687.

15. P. Sudhakar and P. Thilagar, *J. Chem. Sci.*, 2013, **125**, 41-49.

16. a) Bruker (2005). SAINT Version 7.23a. Bruker AXS Inc., Madison, Wisconsin, USA; b) Bruker (2006). APEX 2 Version 2.0-2. Bruker AXS Inc., Madison, Wisconsin, USA; c) G. M. Sheldrick (2008). SADABS. University of Göttingen, Germany.

17. a) G. M. Sheldrick, *Acta Cryst.*, 2008, **A64**, 112-122; b) G. M. Sheldrick, *Acta Cryst.*, 2015, **C71**, 3-8.

18. S. Grimme, *J. Comput. Chem.*, 2006, **27**, 1787-1799.

19. Gaussian 09, Revision A.02, M. J. Frisch, G. W. Trucks, H. B. Schlegel, G. E. Scuseria, M. A. Robb, J. R. Cheeseman, G. Scalmani, V. Barone, G. A. Petersson, H. Nakatsuji, X. Li, M. Caricato, A. Marenich, J. Bloino, B. G. Janesko, R. Gomperts, B. Mennucci, H. P. Hratchian, J. V. Ortiz, A. F. Izmaylov, J. L. Sonnenberg, D. Williams-Young, F. Ding, F. Lipparini, F. Egidi, J. Goings, B. Peng, A. Petrone, T. Henderson, D. Ranasinghe, V. G. Zakrzewski, J. Gao, N. Rega, G. Zheng, W. Liang, M. Hada, M. Ehara, K. Toyota, R. Fukuda, J. Hasegawa, M. Ishida, T. Nakajima, Y. Honda, O. Kitao, H. Nakai, T. Vreven, K. Throssell, J. A. Montgomery, Jr., J. E. Peralta, F. Ogliaro, M. Bearpark, J. J. Heyd, E. Brothers, K. N. Kudin, V. N. Staroverov, T. Keith, R. Kobayashi, J. Normand, K. Raghavachari, A. Rendell, J. C. Burant, S. S. Iyengar, J. Tomasi, M. Cossi, J. M. Millam, M. Klene, C. Adamo, R. Cammi, J. W. Ochterski, R. L. Martin, K. Morokuma, O. Farkas, J. B. Foresman, and D. J. Fox, Gaussian, Inc., Wallingford CT, 2009.

20. X. Cao and M. Dolg, *J. Chem. Phys.*, 2001, **115**, 7348-7355.

21. M. Dolg, U. Wedig, H. Stoll and H. Preuss, *J. Chem. Phys.*, 1987, **86**, 866-872.

22. D. Andrae, U. Haussermann, M. Dolg, H. Stoll and H. Preuss, *Theor. Chim. Acc.*, 1990, **77**, 123-141.

23. D. Figgen, G. Rauhut, M. Dolg and H. Stoll, *Chem. Phys.*, 2005, **311**, 227-244.

24. Basis sets were obtained from the Extensible Computational Chemistry Environment Basis Set Database, Version 1.2.2 [https://bse.pnl.gov/bse/portal]. a) The Role of Databases in Support of Computational Chemistry Calculations, D. Feller, J. Comp. Chem. 1996, 17, 1571–1586. b) Basis Set Exchange: A Community Database for Computational Sciences, K. L. Schuchardt, B. T. Didier, T. Elsethagen, L. Sun, V. Gurumoorthi, J. Chase, J. Li T. L. Windus, J. Chem. Inf. Model. 2007, 47, 1045–1052.

25. E. D. Glendening, A. E. Reed, J. E. Carpenter, F. Weinhold, NBO, Version 3.1.

26. AIMAll (Version 17.01.25), T. A. Keith, TK Gristmill Software, Overland Park KS, USA, 2017 (aim.tkgristmill.com).

27. a) M. A. Bennett, M. Contel, D. C. R. Hockless and L. L. Welling, *Chem. Commun.*, 1998, 2401-2402; b) M. A. Bennett, M. Contel, D. C. R. Hockless, L. L. Welling and A. C. Willis, *Inorg. Chem.*, 2002, **41**, 844-855.

28. E. Hupf, E. Lork, S. Mebs and J. Beckmann, *Inorg. Chem.*, 2015, **54**, 1847-1859.

29. M. Mantina, A. C. Chamberlin, R. Valero, C. J. Cramer and D. G. Truhlar, *J. Phys. Chem. A*, 2009, **113**, 5806-5812.

30. S. S. Batsanov, *J. Mol. Struc.-Theochem*, 1999, **468**, 151-159.

31. a) M. Kranenburg, P. C. J. Kamer and P. W. N. M. van Leeuwen, *Eur. J. Inorg. Chem.*, 1998, 155-157; b) D. S. B. Daniels, A. S. Jones, A. L. Thompson, R. S. Paton and E. A. Anderson, *Angew. Chem. Int. Ed.*, 2014, **53**, 1915-1920; c) L. P. Wolters, W. J. van Zeist and F. M. Bickelhaupt, *Chem. - Eur. J.*, 2014, **20**, 11370-11381; d) L. P. Wolters, R. Koekkoek and F. M. Bickelhaupt, *ACS Catal.*, 2015, **5**, 5766-5775; e) Y. Z. Jiao, M. S. Torne, J. Gracia, J. W. Niemantsverdriet and P. W. N. M. van Leeuwen, *Catal. Sci. Technol.*, 2017, **7**, 1404-1414.

32. a) W. L. Steffen and G. J. Palenik, *Inorg. Chem.*, 1976, **15**, 2432-2438; b) T. Hayashi, M. Konishi, Y. Kobori, M. Kumada, T. Higuchi and K. Hirotsu, *J. Am. Chem. Soc.*, 1984, **106**, 158-163.

33. a) L. R. Falvello, J. Fornies, A. Martin, R. Navarro, V. Sicilia and P. Villarroya, *Inorg. Chem.*, 1997, **36**, 6166-6171; b) L. R. Falvello, S. Fernandez, R. Navarro and E. P. Urriolabeitia, *Inorg. Chem.*, 1999, **38**, 2455-2463; c) M. Kim, T. J. Taylor and F. P. Gabbaï, *J. Am. Chem. Soc.*, 2008, **130**, 6332-6333; d) S. Sharma, R. S. Baligar, H. B. Singh and R. J. Butcher, *Angew. Chem. Int. Ed.*, 2009, **48**, 1987-1990.

TOC Entry

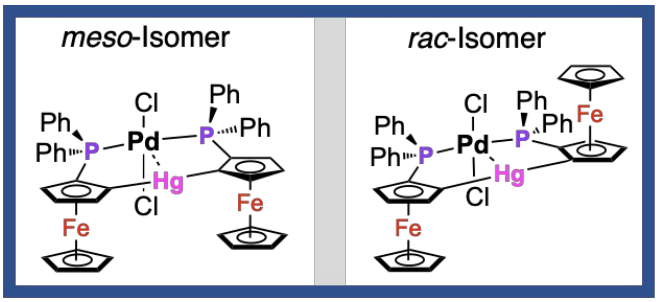

Two isomeric diphosphine chelate ligands with divergent orientation of the ferrocenes were prepared independently and their complexation to Pd(II) investigated.